Solid State Phenomena
ISSN: 1662-9779, Vol. 342, pp 85-89
doi:10.4028/p-6jg806

Submitted: 2022-08-31
Revised: 2022-11-23
Accepted: 2022-11-25
Online: 2023-05-25

Exploring UV-Laser Effects on Al-Implanted 4H-SiC

Marilena Vivovna[1,a*], Filippo Giannazzo[1,b], Gabriele Bellocchi[2,c], Salvatore Ethan Panasci[1,3,d], Simonpietro Agnello[1,4,5,e], Paolo Badalà[2,f], Anna Bassi[2,g], Corrado Bongiorno[1,h], Salvatore Di Franco[1,i], Simone Rascunà[2,j] and Fabrizio Roccaforte[1,k]

[1]CNR-IMM, Strada VIII n.5, Zona Industriale, I-95121, Catania, Italy

[2]STMicroelectronics, Stradale Primosole 50, I-95121, Catania, Italy

[3]Department of Physics and Astronomy, University of Catania, Via Santa Sofia 64, I-95123 Catania, Italy

[4]Department of Physics and Chemistry Emilio Segrè, University of Palermo, via Archirafi 36, I-90123 Palermo, Italy

[5]ATEN Center, University of Palermo, Viale delle Scienze Ed. 18, I-90128 Palermo, Italy

[a] *marilena.vivona@imm.cnr.it, [b]filippo.giannazzo@imm.cnr.it, [c]gabriele.bellocchi@st.com, [d]salvatoreethan.panasci@imm.cnr.it, [e]simonpietro.agnello@unipa.it, [f]paolo.badala@st.com, [g]anna.bassi@st.com, [h]corrado.bongiorno@imm.cnr.it, [i]salvatore.difranco@imm.cnr.it, [j]simone.rascuna@st.com, [k]fabrizio.roccaforte@imm.cnr.it

Keywords: 4H-SiC, Al-implantation, laser annealing treatment, dopant activation

Abstract. In this paper, we explore the effects of excimer laser irradiation on heavily Aluminum (Al)-implanted silicon carbide (4H-SiC) layer. 4H-SiC layers were exposed to UV-laser radiation (308 nm, 160 ns), at different laser fluences and the effects of the laser exposure surface were evaluated from morphological, micro-structural and nano-electrical standpoints. Depending on the irradiation condition, significant near-surface changes were observed. Moreover, the electrical characteristics of the implanted layer, evaluated by means of transmission line method, gave a sheet-resistance of 1.62×10^4 kΩ/sq for the irradiated layer, linked to a poor activation of the p-type dopant and/or a low mobility of the carriers in the laser-modified 4H-SiC layer. This study can be useful for a fundamental understanding of laser annealing treatments of 4H-SiC implanted layers.

Introduction

Today, silicon carbide (4H-SiC) Schottky diodes and metal oxide semiconductor field effect transistors (MOSFETs) have reached a high level of technological maturity and are commercially employed in power electronics applications [1]. However, many research activities are still devoted to the device performance improvement, in order to achieve the full benefits offered by 4H-SiC material. As an example, the optimization of specific device processing phases can enable an amelioration of the device characteristics. In particular, the ion-implantation technique is the consolidated method for selective doping in 4H-SiC power electronics devices, such as junction barrier Schottky diodes or MOSFETs [2]. Nonetheless, some drawbacks are present, with ion-implantation that inevitably leads to the production of lattice damage or even amorphization of the material [3] and post-implantation thermal annealing treatments are required to partially restore the crystalline structure of the semiconductor [4] and achieve the electrical activation of the dopant species [2]. Typically, these annealing treatments are carried out in conventional furnaces at high temperature (>1600°C), and this process can generate defects, which are in turn detrimental for the electrical activation of the dopant [5].

Among all the explored unconventional rapid thermal annealing treatments [6,7,8,9], pulsed-laser annealing methods supply many advantages, as they provide extremely fast heating ramps and allow to locally reach much higher temperatures than the conventional furnace annealing treatment. Furthermore, laser-annealing treatment offers a high localization (up to micrometric scale),

compatibility with wafer-scale processing and can simplify 4H-SiC devices fabrication by the possibility to pattern the laser beam arriving on the sample surface. In this work, we explore the effects of pulsed UV-laser annealing treatment on Al-implanted 4H-SiC layers. The combination of various morphological, structural and electrical characterization techniques provided a wide picture of the modification induced by the laser exposure of the material.

Experimental Details

An n-type 4H-SiC epitaxial layer was implanted at 500°C with A-ions, using doses and energies in order to achieve an Al-ion profile with high concentration (up to 1×10^{20} at/cm^3) and extended over 300 nm. Different dies were cut from the wafer and exposed to few pulses (up to four) of an excimer (XeCl)-laser radiation (308 nm, 160 ns, 4Hz), at comparatively low fluence (1.4 and 1.6 J/cm^2) or high fluence (2.4 and 2.6 J/cm^2), as sketched in Fig.1. The laser-induced effects on the morphological and microstructural properties of the exposed surface were studied, as well as on the electrical properties of the implanted layer. Specifically, the surface morphology was investigated by Atomic Force Microscopy (AFM) in sample regions of 10μm×10μm. In the same areas, the local current conduction was evaluated by conductive-AFM (C-AFM) technique. The microstructural laser-induced modifications were assessed by Transmission Electron Microscopy (TEM) technique. Finally, the electrical properties of the laser-irradiated Al-implanted layers were determined by current-voltage-temperature (I-V-T) measurements on appropriate structures, based on circular Transmission Line Model (C-TLM) [10] with a Ti(10nm)/Ni(100nm) stack as contact, annealed at 950°C in N_2 for 60 sec.

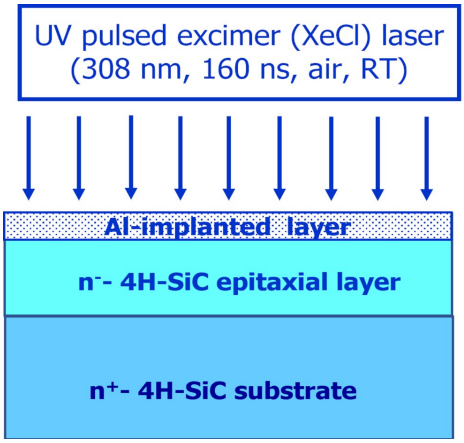

Fig.1: Cross-section view of the Al-implanted 4H-SiC sample under excimer (XeCl) laser irradiation.

Results and Discussion

Firstly, we monitored the evolution of the morphology (by AFM) and local current conduction (by C-AFM) following the laser exposure. Fig.2 reports the features of the 4H-SiC surface in the as-implanted and laser-irradiated samples at 1.6 and 2.4 J/cm^2. Clearly, we observed that the initial morphology (Fig.2a) changed, with the appearance of micrometer-size features that increasingly overlap the original steps (Figs.2b and 2c). At the same time, the laser-irradiation induced an increase of the local current (Figs.2d and 2e) up to a saturation condition for the highest fluence irradiated sample (Fig.2f).

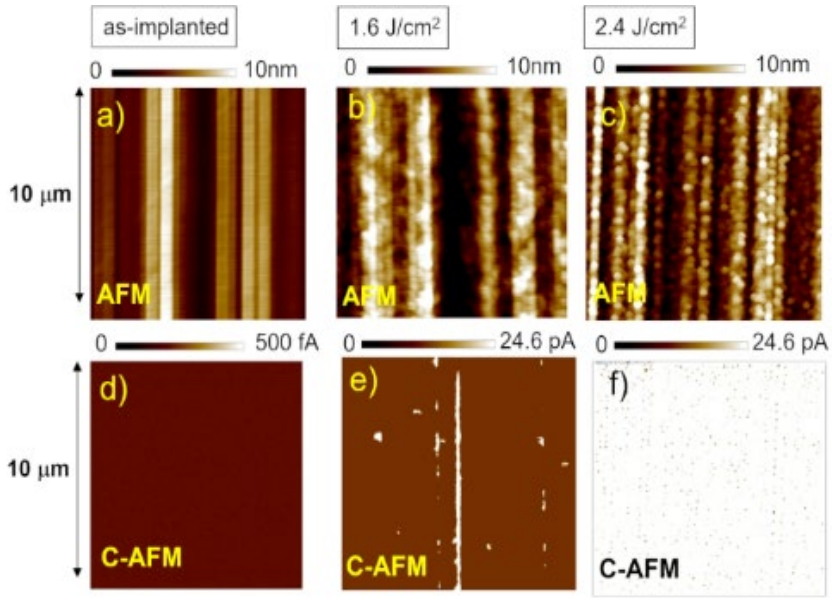

Fig. 2. AFM micrographs (*a*, *b* and *c*) and associated C-AFM current maps (*d*, *e* and *f*) acquired on the 4H-SiC layer in as-implanted sample and laser irradiated samples.

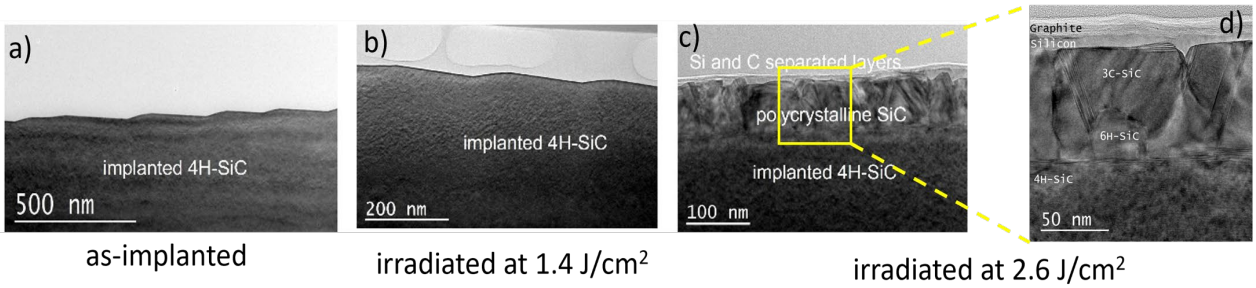

Fig. 3. Cross-section TEM images of 4H-SiC layer *a)* as-implanted, *b)* irradiated at 1.4 J/cm^2 and *c)* at 2.6 J/cm^2. *d)* High magnification images of an area of the highest fluence irradiated sample (from *c*).

Cross-sectional TEM analyses provided insights on the laser-induced changes in the microstructural properties. Fig.3 compares the TEM images of three Al-implanted samples, consisting of the as-implanted sample and two samples irradiated at 1.4 and 2.6 J/cm^2. Specifically, the low-fluence irradiated 4H-SiC layer (Fig. 3b) does not show any significant modification with respect to the as-implanted sample (Fig.3a). Instead, in the high-fluence irradiated sample a very different surface was observed (Fig.3c), with an about 100nm-thick polycrystalline layer. On top of this layer, we observed in the order a crystalline-silicon layer and a carbon-rich region, as also confirmed by Raman analysis (not shown here). In particular, focusing on this part with high magnified analysis as shown in Fig.3d, form the analysis of the diffraction patterns (not-reported here), it was possible to conclude that the polycrystalline layer consisted in a combination of 3C-SiC and 6H-SiC grains. The presence of the conductive carbon region in the uppermost part of the sample is the main cause of the strong increase in the vertical injected current observed in the C-AFM maps (Fig 2). The electrical properties of the 4H-SiC Al-implanted layer after laser-irradiation were also evaluated by means of C-TLM test patterns fabricated using Ti/Ni contacts (as shown in Fig.4a). Before the electrical characterization, the upper carbon-rich and Si layers were removed by an oxidation process at 800°C for 60min following by wet etching (in diluted HF solution). The electrical analysis was performed on three different samples irradiated at 1.6 and 2.0 and at 2.4 J/cm^2. However, only sample irradiated at 2.4 J/cm^2 presented linear I-V curves scaling with the pad distance variation, reported in Fig.4b. From the slope of these I-V characteristics, acquired at measurement temperature varying from 298 to 398 K, the total resistance R_{TOT} values were derived, resulting in the order of hundreds of kΩ (Fig.5a). The linear dependence of the R_{TOT} on the pad interdistance allowed the determination of the sheet

resistance R_{SH} of the layer. Fig. 5b shows the R_{SH} values for the laser-irradiated Al-implanted layer as a function of the measurement temperature: R_{SH} decreased from 1.62×10^4 kΩ/sq (at room temperature) down to 3.18×10^3 kΩ/sq (at 125°C). Noteworthy, this trend of the R_{SH} with temperature is peculiar of doped semiconductors. Fig.5c presents an Arrhenius' plot of the R_{SH} values in this system, from which we extrapolated an activation energy of about 166 meV, peculiar of the system under investigation. In fact, this value can be interpreted as an effective ionization energy for Al-ion in a polycrystalline SiC layer, i.e. formed by 3C and 6H regions. Furthermore, it was possible to estimate a value of the resistivity of this layer ρ=160 Ω×cm at room temperature. This value is significantly higher than the typical values measured in a 4H-SiC sample implanted under the same conditions but subjected to conventional thermal annealing [11]. Thus, we can suppose that in this complex system a low level of electrical activation for the Al-ions and/or a poor mobility of the carriers in the polycrystalline layer occurred.

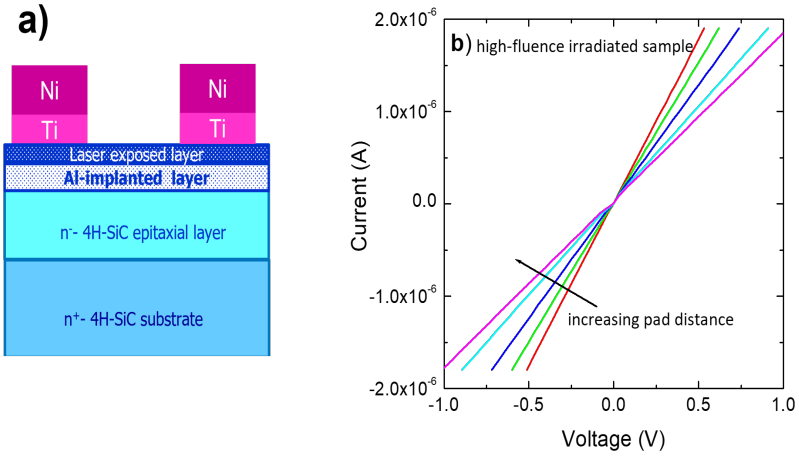

Fig. 4. *a)* Cross-section view of the Ni/Ti contacts fabricate on the laser exposed sample, after removal of the most external layers (Si and C -rich layers). *b)* I–V curves acquired on a set of C-TLM for the sample irradiated at 2.4 J/cm^2 curves.

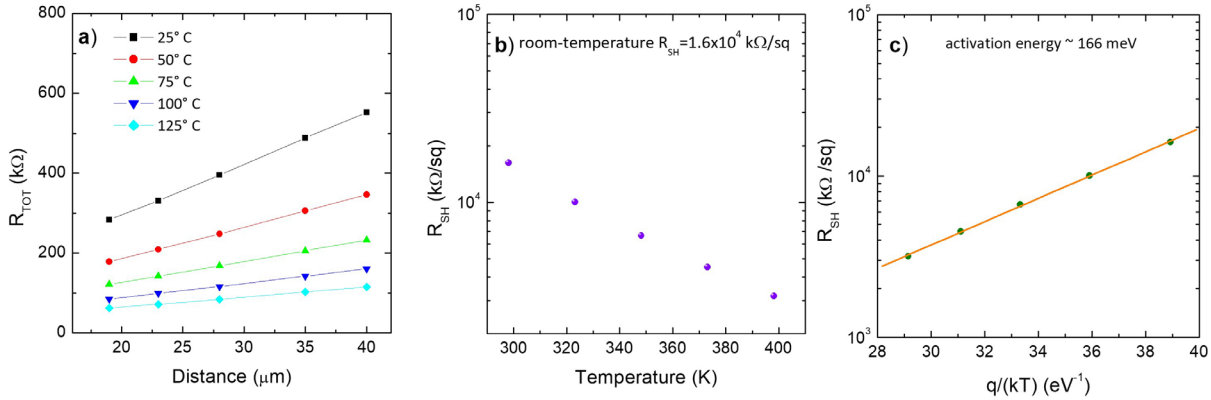

Fig. 5. *a)* R_{TOT} extrapolated from the slope of the I-V characteristics acquired at measurement temperature varying from 298 to 398 K. *b)* Temperature-dependence of the sheet resistance R_{SH} in the sample irradiated at 2.4 J/cm^2 and *c)* related Arrhenius' plot R_{SH} *vs* q/kT for the activation energy derivation.

Summary

In this work, we have studied the effects UV excimer laser-irradiation on Al-implanted 4H-SiC layers. The effects for different fluences were evaluated from a morphological, microstructural, and electrical standpoints. In particular, the evolution of the surface morphology and local current conduction observed with increasing the laser fluence, was explained by the formation of a C- and Si-rich layers

over a polycrystalline region with 3C and 6H-SiC grains. From the electrical analysis of the implanted layer, performed after the removal of the external conductive layers, we observed a decreasing of the sheet resistance with increasing the measurement temperature, as typically observed for the p-type doped material. Nevertheless, we obtained a resistivity significantly higher than that observed in similar samples subjected to conventional annealing process, related to the complex system formed after laser irradiation, with the occurrence either a poor electrical activation or a low carrier mobility.

References

[1] T. Kimoto, Jpn. J. Appl. Phys. 54 (2015) 040103.

[2] F. Roccaforte, P. Fiorenza, M. Vivona, G. Greco, F. Giannazzo, Materials 14 (2021) 3923 1-24.

[3] B.G. Svensson, A. Hallén, M. K. Linnarsson, A. Y. Kuznetsov, M. S. Janson, B. Formanek, J. Österman, P. O. Persson, L. Hultman, L. Storasta, F. H. C. Carlsson, P. Bergman, C. Jagadish, E. Morvan, Mater. Sci. Forum 353-356 (2001) 549-554.

[4] A. Hedler, S. Urban, F. Falk, H. Hobert, W. Wesch, Appl. Surf. Sci. 205 (2003) 240-248.

[5] E. Wendler, A. Heft, W. Wesh, Nucl. Instr. Meth. Phys. B 141 (1998) 105.

[6] S. G. Sundaresan. M. V. Rao, Y. Tian, M. C. Ridgway, J. A. Schreifels, J. J. Kopanski, J. Appl. Phys. 101 (2007) 073708 1-7.

[7] K. Maruyama, H. Hanafusa, R. Ashihara, S. Hayashi, H. Murakami, S. Higashi, Jpn. J. Appl. Phys. 54 (2015) 06GC01 1-8.

[8] C. Dutto, E. Fogarassy, D. Mathiot, D. Muller, P. Kern, D. Ballutaud, Appl. Surf. Sci. 208-209 (2003) 292-297.

[9] M. Vivona, F. Giannazzo, G. Bellocchi, S. E. Panasci, S. Agnello, P. Badalà, A. Bassi, C. Bongiorno, S. Di Franco, S. Rascinà, F. Roccaforte, ACS Appl. Electron. Mater. 4 (2022) 4514-4520.

[10] Schroder, D.K. Semiconductor Material and Device Characterization, 3rd Ed.; John Wiley & Sons Inc.: Hoboken, NJ, USA, 2006.

[11] M. Spera, G. Greco, D. Corso, S. Di Franco, A. Severino, A. A. Messina, F. Giannazzo, F. Roccaforte, Materials 12 (2019) 3468 1-9.